Instability of Flow in Magnetic Nozzle

Hunt Feng

June 27, 2023

Contents

1 Introduction **2**
- 1.1 Linear Instability of Plasma Flow . . . 2
- 1.2 Flow in Magnetic Nozzle . . . 2
  - 1.2.1 Magnetic Field in Magnetic Nozzle . . . 3
- 1.3 Governing Equations for Flow in Magnetic Nozzle . . . 4
  - 1.3.1 Velocity Profile at Equilibrium . . . 5
- 1.4 Linearized Equations . . . 6
- 1.5 Polynomial Eigenvalue Problem . . . 6
- 1.6 Goal of this Thesis . . . 6

2 Spectral Method and Spectral Pollution **7**
- 2.1 Spectral Method . . . 7
- 2.2 Spectral Pollution and Spurious Modes . . . 7
  - 2.2.1 Illustration: Constant velocity case . . . 7

3 Singular Perturbation **10**
- 3.1 Existence of Singularity . . . 10
  - 3.1.1 Singularity and Black hole . . . 10
- 3.2 Boundary Condition at a Singular Point . . . 11
- 3.3 Shooting Method . . . 12
  - 3.3.1 Result . . . 12

4 Future Work **14**

A Numerical Experiments **16**
- A.1 Constant Velocity Case - Subsonic . . . 16
- A.2 Constant Velocity Case - Supersonic . . . 17
- A.3 Error . . . 17
- A.4 Subsonic Case . . . 18
- A.5 Supersonic Case . . . 19
- A.6 Accelerating Case . . . 19

B Spectral Pollution: Analysis of Numerical Spectrum **20**

Chapter 1

Introduction

1.1 Linear Instability of Plasma Flow

The instability of plasma flow refers to the tendency of a plasma system to deviate from a stable, equilibrium state and exhibit perturbations or fluctuations in its behavior.[2] A mechanical analogy is shown in Fig.1.1. These instabilities can arise from various factors, such as the interaction of particles with electromagnetic fields, collective effects, or the presence of gradients in plasma parameters.

To study the linear instability of a configuration, one can linearize the equations of motion for small deviations from an equilibrium state. [2] By assuming the perturbations are oscillatory, meaning that it is proportional to $\exp(-i\omega t)$ and substituting into the linearized equations, one obtains the equations about the frequency ω. Solving for ω we can examine the instability of of the problem.

- If the frequency has positive imaginary part, $\mathrm{Im}(\omega) > 0$, the plasma flow is unstable since the perturbed quantities grows exponentially in time, $\exp(\mathrm{Im}(\omega)t)$.
- If the frequency has negative imaginary part, $\mathrm{Im}(\omega) < 0$, the plasma flow is stable since the perturbations decays over time.
- If $\mathrm{Im}(\omega) = 0$, then the plasma flow is also stable.

Therefore, the imaginary part of ω, $\mathrm{Im}(\omega)$, is often called growth rate of instability.

Figure 1.1: Mechanical analogy of various types of equilibrium. Adapted from [2].

Plasma flow in magnetic mirror configurations have been studied extensively in plasma physics due to its frequent precense in many areas such as the accretion flow [5, 1], and magnetic nozzle[8]. However, the stability of these configurations remains a debatable subject. In this research, we will focus on the linear instability of the plasma flow in magnetic nozzle.

1.2 Flow in Magnetic Nozzle

A magnetic nozzle is a device that uses a magnetic field to shape and control the flow of charged particles in a plasma propulsion system, see Fig.1.2. By employing the magnetic mirror configuration, the magnetic nozzle

can effciently direct and accelerate the plasma flow, generating thrust for propulsion. The magnetic field in the nozzle helps collimate and focus the plasma exhast, increasing its velocity and enhancing the performance of the propulsion system. However, instabilities can develop and potentially affect the performance of magnetic nozzle. [6]

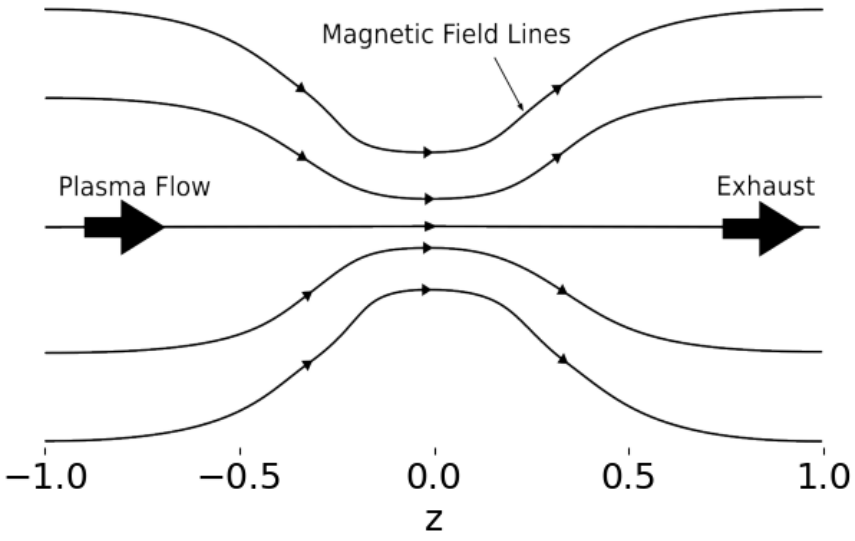

Figure 1.2: A simplified model of the magnetic nozzle

1.2.1 Magnetic Field in Magnetic Nozzle

In 1D problem, the magnetic field can be modeled as

$$B(z) = B_0 \left[1 + R \exp\left(-\left(\frac{x}{\delta}\right)^2\right)\right]$$

where $1 + R$ is the magnetic mirror ratio, and δ determines the spread of the magnetic field. It is shown in Fig.(1.3).

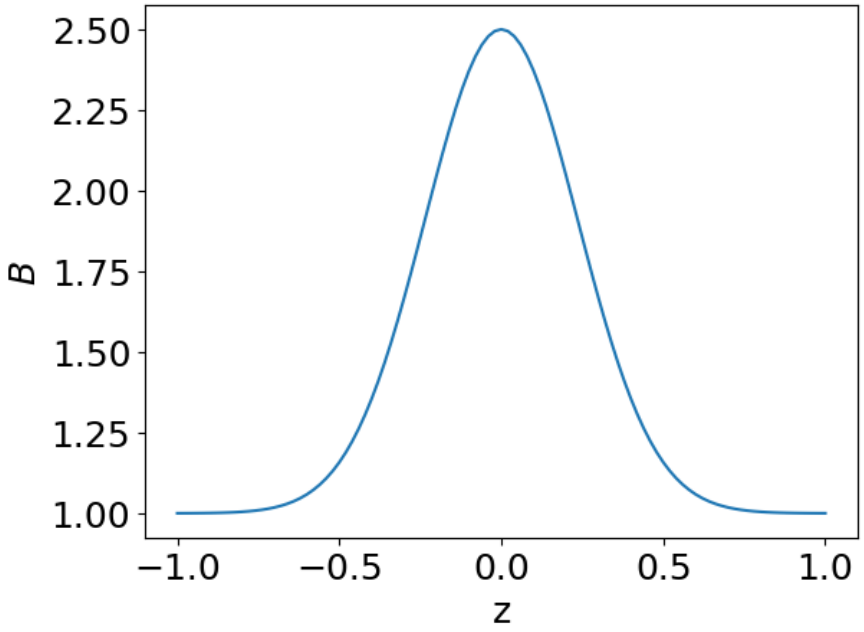

Figure 1.3: This is the magnetic field in nozzle with mirror ratio $1 + R = B_{max}/B_{min} = 2.5$, and the spread of magnetic field, $\delta = 0.1/0.3 = 0.\bar{3}$.

1.3 Governing Equations for Flow in Magnetic Nozzle

In this section, we will derive the governing equations of the flow in magnetic nozzle, starting from the fluid description for plasma.

In magnetic nozzle, the magnetic field is along the nozzle, which we denote as z-axis. Due to Lorentz force, the charged particles gyrates about the magnetic field lines. Because the magnetic moment is invariant in such situation (**reference**). The fluid velocity of particles can be written as $\mathbf{v} = v\mathbf{B}/B$, meaning that the particles move along the magnetic field lines. Therefore the conservation of density

$$\frac{\partial n}{\partial t} + \boldsymbol{\nabla} \cdot (n\mathbf{v}) = 0 \Rightarrow \frac{\partial n}{\partial t} + B\frac{\partial}{\partial z}\left(\frac{nv}{B}\right) = 0$$

In the derivation, $\boldsymbol{\nabla} \cdot \mathbf{B} = 0$ is used.

To derive the second governing equation, we start from the conservation of momentum,

$$\frac{\partial v}{\partial t} + v\frac{\partial v}{\partial z} = -\frac{1}{\rho}\boldsymbol{\nabla} p$$

Let $\boldsymbol{\nabla} p = k_B T \, \partial n/\partial z$, we have

$$\frac{\partial v}{\partial t} + v\frac{\partial v}{\partial z} = -c_s^2 \frac{1}{n}\frac{\partial n}{\partial z}$$

where $c_s^2 = k_B T/m$ is the square of sound speed.

Therefore the dynamics of the flow in magnetic nozzle can be characterized by the conservation of density and momentum,

$$\frac{\partial n}{\partial t} + B\frac{\partial}{\partial z}\left(\frac{nv}{B}\right) = 0 \tag{1.1}$$

$$\frac{\partial v}{\partial t} + v\frac{\partial v}{\partial z} = -c_s^2 \frac{1}{n}\frac{\partial n}{\partial z} \tag{1.2}$$

1.3.1 Velocity Profile at Equilibrium

Let n_0 and v_0 be the density and velocity at equilibrium (stationary solution). Substitute them into Eq.(1.1) and Eq.(1.2), we get the so-called equilibrium condition which n_0 and v_0 must satisfy,

$$\frac{\partial}{\partial z}\left(\frac{n_0 v_0}{B}\right) = 0$$
$$v_0 \frac{\partial v_0}{\partial z} = -c_s^2 \frac{1}{n_0}\frac{\partial n_0}{\partial z}$$

Let $M(z) = v_0(z)/c_s$ be the Mach number (nondimensionalized velocity). We can express M using the Lambert W function,

$$M(z) = \left[-W_k\left(-\frac{B(z)^2}{B_m^2} M_m^2 e^{-M_m^2}\right)\right]^{1/2}$$

where the subscript k of W stands for branch of Lambert W function. When $k = 0$, it is the subsonic branch; When $k = -1$, it is the supersonic branch. Below shows a few cases of the solution.

- $M_m < 1, k = 0$, subsonic velocity profile.
- $M_m = 1$, $k = 0$ for $x < 0$ and $k = -1$ for $x > 0$, accelerating profile
- $M_m = 1$, $k = -1$ for $x < 0$ and $k = 0$ for $x > 0$, decelerating profile
- $M_m > 1, k = -1$, supersonic velocity profile

Fig.(1.4) shows some cases of the solution.

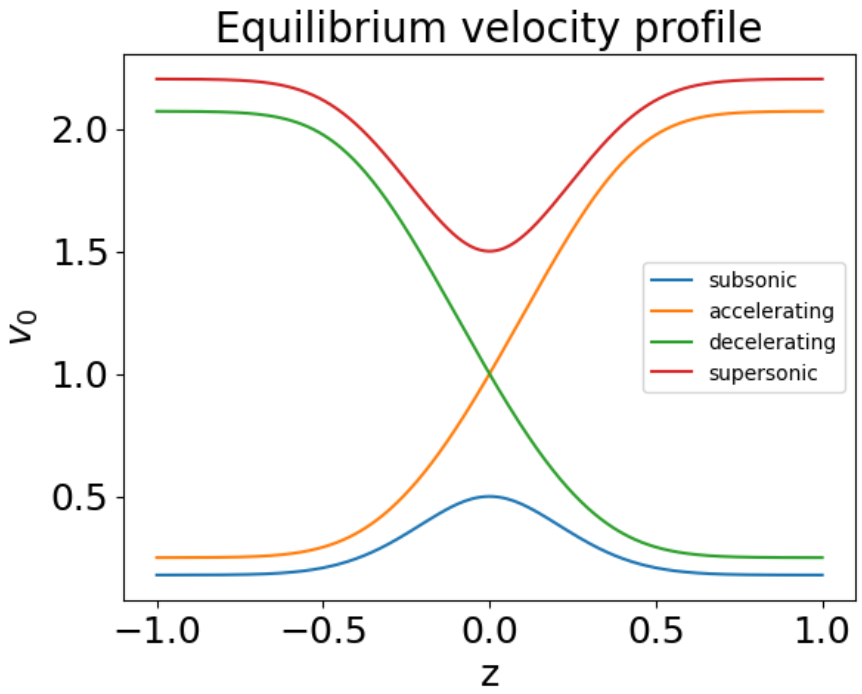

Figure 1.4: The velocity profile in the magnetic nozzle is completely determined by M_m, the velocity at the midpoint, $z = 0$. For the transonic velocity profiles, M_m alone is not enough to determine the profile, we need to specify the branch of Lambert W function to determine whether it is accelerating or decelerating.

1.4 Linearized Equations

For convenience, we nondimensionalize the governing equations by normalizing the velocity to c_s, $v \mapsto v/c_s$, z to system length L, $z \mapsto z/L$ and time $t \mapsto c_s t/L$. The governing equations become

$$\frac{\partial n}{\partial t} + n\frac{\partial v}{\partial z} + v\frac{\partial n}{\partial z} - nv\frac{\partial_z B}{B} = 0 \tag{1.3}$$

$$n\frac{\partial v}{\partial t} + nv\frac{\partial v}{\partial z} = -\frac{\partial n}{\partial z} \tag{1.4}$$

and the nondimensionalized equilibrium condition is

$$\frac{\partial}{\partial z}\left(\frac{n_0 v_0}{B}\right) = 0 \tag{1.5}$$

$$v_0\frac{\partial v_0}{\partial z} = -\frac{1}{n_0}\frac{\partial n_0}{\partial z} \tag{1.6}$$

Now we are going to derive an important intermediate result, the linearized governing equations. Let $n = n_0(z) + \tilde{n}(z,t)$ and $v = v_0(z) + \tilde{v}(z,t)$, where $\tilde{n}$ and $\tilde{v}$ are small perturbed quantities. The linearized governing equations are

$$\frac{1}{n_0}\frac{\partial \tilde{n}}{\partial t} + \frac{\partial \tilde{v}}{\partial z} + v_0\tilde{Y} + \tilde{v}\frac{\partial_z n_0}{n_0} - \tilde{v}\frac{\partial_z B}{B} = 0 \tag{1.7}$$

$$\frac{\partial \tilde{v}}{\partial t} + \frac{\partial(v_0\tilde{v})}{\partial z} = -\tilde{Y} \tag{1.8}$$

where

$$\tilde{Y} \equiv \frac{1}{n_0}\frac{\partial \tilde{n}}{\partial z} - \frac{\partial_z n_0}{n_0^2}\tilde{n} = \frac{\partial}{\partial z}\left(\frac{\tilde{n}}{n_0}\right)$$

1.5 Polynomial Eigenvalue Problem

In order to investigate the instability of magnetic nozzle, we need formulate it as an eigenvalue problem. To do that, we assume the perturbed density and velocity are oscillatory, i.e. $\tilde{n}, \tilde{v} \sim \exp(-i\omega t)$, where ω is the oscillation frequency of the perturbed quantities. This frequency can be a complex number. If $\omega = \omega_r + i\omega_i$, then the perturbed quantities becomes $\tilde{n} \sim \exp(\omega_i t)\exp(i\omega_r t)$, which means it grows exponentially with time.

Let $\tilde{n} \sim \exp(-i\omega t)$ and $\tilde{v} \sim \exp(-i\omega t)$, then we have the polynomial eigenvalue problem

$$\begin{aligned} &\omega^2\tilde{v} \\ &+2i\omega\left(v_0\frac{\partial}{\partial z} + \frac{\partial v_0}{\partial z}\right)\tilde{v} \\ &+\left[(1-v_0^2)\frac{\partial^2}{\partial z^2} - \left(3v_0 + \frac{1}{v_0}\right)\frac{\partial v_0}{\partial z}\frac{\partial}{\partial z} - \left(1 - \frac{1}{v_0^2}\right)\left(\frac{\partial v_0}{\partial z}\right)^2 - \left(v_0 + \frac{1}{v_0}\right)\frac{\partial^2 v_0}{\partial z^2}\right]\tilde{v} = 0 \end{aligned} \tag{1.9}$$

1.6 Goal of this Thesis

The goal of this thesis is to study the instabilities of the magnetic mirror configuration given certain boundary conditions and equilibrium velocity profiles.

To achieve the goal, first we need to study the spectral method for solving the instability problem. To use spectral method, it is necessary to understand different discretizations of the operators, such as finite difference, finite element and spectral element method.

Once the spectral method is introduced, we can use it to study the instability of plasma flow in magnetic nozzle as an eigenvalue problem. We can obtain results by using different discretization techniques. By comparing the results from different approach, we can increase the credibility of the true solution.

However, spectral method is not suitable when the equilibrium velocity profile is transonic due to the precense of singularity at the sonic point. We need to solve the singular perturbation problem around the singularity analytically. Then starting from the singular point, we can use shooting method to find eigenvalues.

Chapter 2

Spectral Method and Spectral Pollution

2.1 Spectral Method

Spectral method is one of the best tools to solve PDE and ODE problems. [9] The central idea of spectral method is by discretizing the equation, we can transform that to a linear system or an eigenvalue problem.

Here we reformulate the polynomial eigenvalue problem, Eq.(1.9) as the following,

$$\begin{bmatrix} 0 & 1 \\ \hat{M} & \hat{N} \end{bmatrix} \begin{bmatrix} \tilde{v} \\ \omega\tilde{v} \end{bmatrix} = \omega \begin{bmatrix} \tilde{v} \\ \omega\tilde{v} \end{bmatrix} \tag{2.1}$$

where the operators $\hat{M}$ and $\hat{N}$ are defined as

$$\hat{M} = -\left[(1-v_0^2)\frac{\partial^2}{\partial z^2} - \left(3v_0 + \frac{1}{v_0}\right)\frac{\partial v_0}{\partial z}\frac{\partial}{\partial z} - \left(1 - \frac{1}{v_0^2}\right)\left(\frac{\partial v_0}{\partial z}\right)^2 - \left(v_0 + \frac{1}{v_0}\right)\frac{\partial^2 v_0}{\partial z^2}\right]$$

$$\hat{N} = -2i\left(v_0\frac{\partial}{\partial z} + \frac{\partial v_0}{\partial z}\right)$$

This becomes an ordinary algebraic eigenvalue problem if we discretize the operators and the function $\tilde{v}$. In this thesis, finite-difference, finite-element and spectral-element discretizations are used.

2.2 Spectral Pollution and Spurious Modes

In this section, we will discuss an important phenomenon we observe throughout the numerical experiments. It is the phenomenon called spectral pollution. Then we will provide a method to filter these spurious modes.

Spectral pollution refers to the phenomenon which some eigenvalues are not converging to the correct value when the mesh density is increased. When solving eigenvalue problems using spectral methods with finite difference or finite element approximations, spectral pollution might occur. [7]

2.2.1 Illustration: Constant velocity case

We will illustrate the spectral pollution by solving Eq.(1.9) with constant velocity profile, $v_0 = \text{const}$, using spectral method with finite-difference method.

Let $v_0 \neq 1$ be a constant, then Eq.(1.9) becomes

$$\omega^2\tilde{v} + 2i\omega v_0\frac{\partial\tilde{v}}{\partial z} + (1-v_0^2)\frac{\partial^2\tilde{v}}{\partial z^2} = 0 \tag{2.2}$$

The dispersion relation can be obtained by substituting $\tilde{v} \sim \exp(-i\omega t + kx)$ into Eq.(2.2),

$$\omega = k(v_0 \pm 1) \tag{2.3}$$

where k is the wave number. We see that all modes should be stable for $\omega \in \mathbb{R}$.

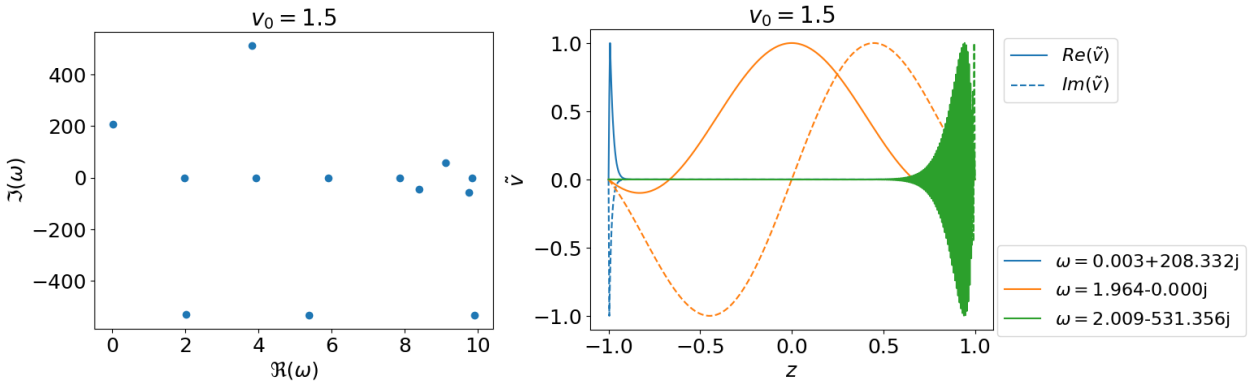

(a) Unfiltered eigenvalues.

(b) First few unfiltered eigenfunctions.

Figure 2.1: Spurious modes occurs when solving Eq.(2.2). Finite difference discretization was used. A considerably high resolution mesh with 501 points was used. In fact, spurious modes occurs regardless of the resolution.

A good way to filter the spurious modes is by doing a convergence test, see Fig.(2.2). Since the eigenvalues, Eq.(B.3), are changing with mesh resolution. We can simply solve the problem using spectral method under different mesh resolution. Then filter out the eigenmodes that are not converging.

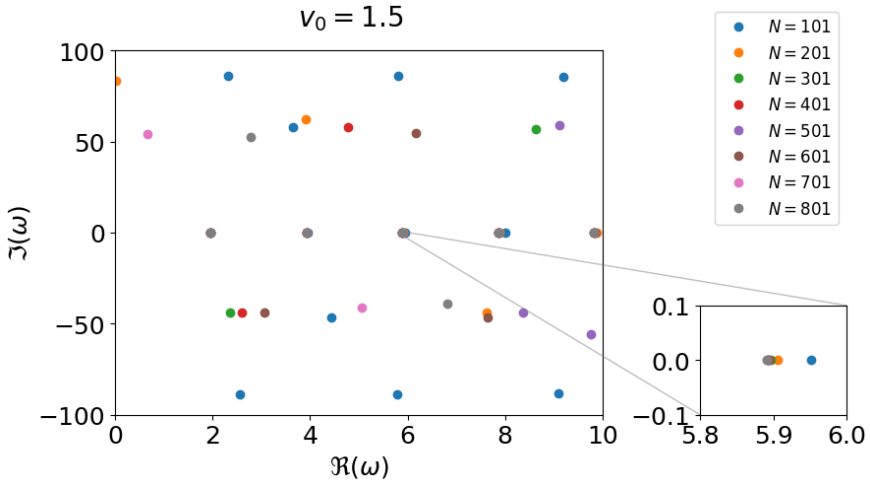

Figure 2.2: Converging test works since spurious eigenvalues change under different resolution. We can see that only the eigenvalues on the real axis are not changing dramatically when resolution increases.

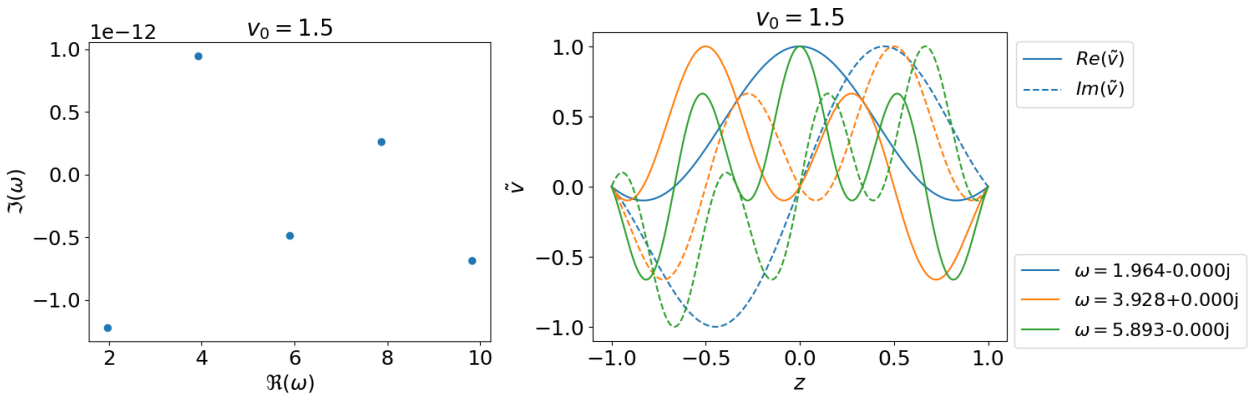

(a) Filtered eigenvalues.

(b) First few filtered eigenfunctions.

Figure 2.3: Filtered spurious modes by converging test.

Chapter 3

Singular Perturbation

3.1 Existence of Singularity

Initially, we thought we can investigate the accelerating case using the same technique. We set up Dirichlet boundary conditions to the problem, and used spectral method with finite difference discretizatin. We found that the eigenfunctions are all squeezed to the center, Fig.3.1.

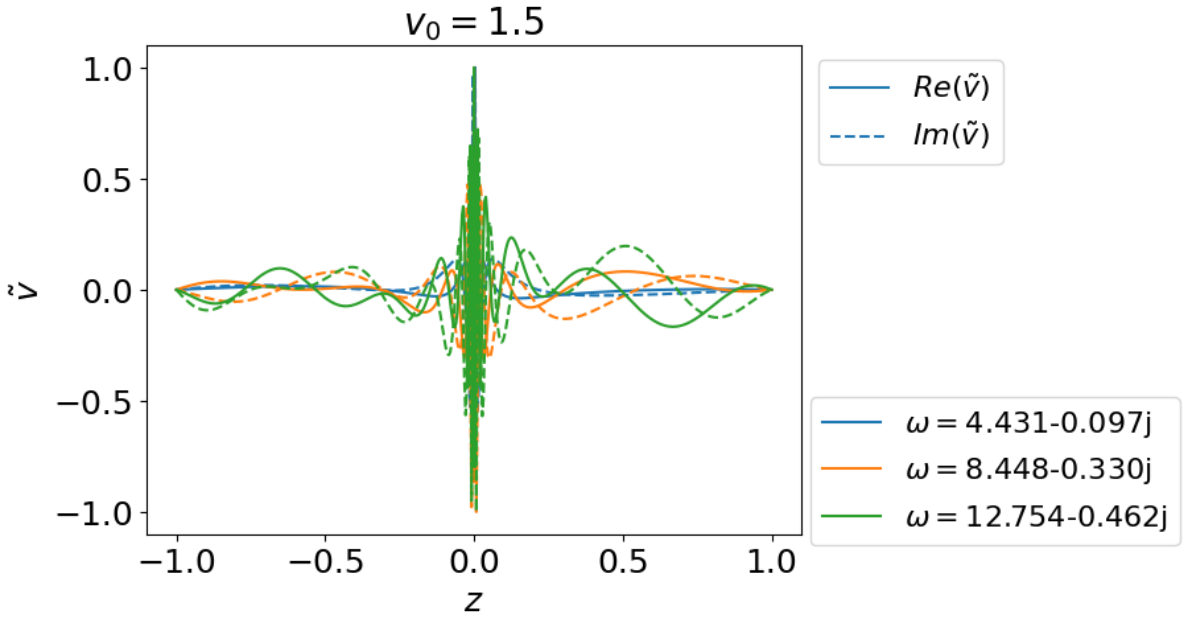

Figure 3.1: Dirichlet boundary conditions are set at the two ends, all eigenfunctions are squeezed to the singular point.

After some investigation, we realized that there is a regular singular point at $z = 0$. It is easy to see that from Eq.(1.9) since the second order derivative term vanishes at $z = 0$ due to the fact that $1 - v_0^2 = 0$ at the sonic point.

3.1.1 Singularity and Black hole

Interesting enough, the acoustic perturbations of the gas fluid flow in the de Laval nozzle are proved to coincide with the quasi-normal modes of black holes solutions deformed by the 5D Weyl fluid. [3, 4] Moreover, the sonic horizon is an exact sonic analogue of black hole horizon. [10]

A quasi-1D fluid flow is ruled by the Euler-Lagrange equations and the continuity relation in fluid mechanics, given by

$$\frac{\partial}{\partial t}(\rho A) + \frac{\partial}{\partial x}(\rho A v) = 0 \tag{3.1}$$

$$\frac{\partial}{\partial t}(\rho A v) + \frac{\partial}{\partial x}[(\rho v^2 + p)A] = 0 \tag{3.2}$$

$$\frac{\partial}{\partial t}\left(\frac{\rho v^2}{2} - \frac{p}{1-\gamma}A\right) + \frac{\partial}{\partial x}\left[\left(\frac{\rho v^2}{2} - \frac{\gamma}{1-\gamma}A\right)Av\right] = 0 \tag{3.3}$$

In [3, 4], the acoustic analogue of tortoise coordinate is introduced,

$$x^* = c_{s0}\int [c_s(x)(1 - M(x)^2)]^{-1} dx$$

where c_{s0} denotes the stagnation speed of sound, $c_s = \mathrm{d}p/\mathrm{d}\rho$ is the local speed of sound and $M(x) = v(x)/c_s(x)$ is the Mach number. Using the tortoise coordinate, the problem can be transformed to a Schrödinger-type equation.

However, there are a few drawbacks in this method.

- This method is complicated, we need to derive the Eq.(1.9) in the new coordinate system.
- The new coordinate system pushes the singularity to infinity. However, we still need to cross the singularity in order to get the eigenvalues if we are using spectral method.

3.2 Boundary Condition at a Singular Point

Some investigation leads us to a better method. To understand the logic flow, we need to realize that the singularity acts as an boundary condition for the problem. That means, we have no freedom to choose the boundary condition on the right once we fixed values of $\tilde{v}$ on the left boundary and at the singularity. We will illustrate this by expanding the solution at the singularity.

If we Taylor expand terms near the singularity, and only keep the first order term for the second order derivative term, Eq.(1.9) becomes

$$-2v_0'(0)z\frac{\partial^2\tilde{v}}{\partial z^2} + (2i\omega - 4v_0'(0))\frac{\partial\tilde{v}}{\partial z} + (\omega^2 + 2i\omega v_0'(0) - 2v_0''(0))\tilde{v} = 0$$

Use Frobenius method, assuming $\tilde{v} = \sum_{n\geq 0} c_n z^{n+r}$, we get two different roots, $r = 0$ and $r = 1-a$. They correspond to finite solution and diverging solution near the singularity, respectively. The coefficients of the power series are given by where

$$\begin{aligned} c_n &= \frac{(-1)^n b^n c_0}{\prod_{k=0}^{n-1}(n + r - k)(n + r - 1 + a - k)} \\ &= (-1)^n b^n c_0 \frac{\Gamma(r+1)\Gamma(r+a)}{\Gamma(n+r+1)\Gamma(n+r+a)} \end{aligned}$$

where

$$a = \frac{2i\omega - 4v_0'(0)}{-2v_0'(0)}; \quad b = \frac{\omega^2 + 2i\omega v_0'(0) - 2v_0''(0)}{-2v_0'(0)}$$

Worth to mention that the diverging solution goes like

$$\tilde{v}(z) \sim z^{1-a} = z^{-1-\omega_i/v_0'(0)} z^{i\omega_r/v_0'(0)}$$

where $\omega = \omega_r + i\omega_i$. Meaning that the solution will be divergent iff $\omega_i > -v'(0)$.

This indicates that the regular solution that crosses the singularity smoothly are determined by two parameters only, c_0 and ω. Once we choose c_0, the perturbation at the singularity, there is only one degree of freedom left, ω. It seems reasonable to set the perturbation to 0 on the left boundary since it is the entrance of the magnetic nozzle. Now there is no more freedom to choose the boundary condition on the exit of the nozzle.

3.3 Shooting Method

Shooting method can be used to solve eigenvalue problem with specified boundary values,

$$g(\tilde{v}(z);\omega) = 0, \quad z_l \le z \le z_r, \quad \tilde{v}(z_l) = \tilde{v}_l, \tilde{v}(z_r) = \tilde{v}_r \tag{3.4}$$

where ω is the eigenvalue to be solved.

Suppose a eigenvalue problem can be formulated as

$$\frac{\mathrm{d}}{\mathrm{d}z}\mathbf{u} = \mathbf{f}(\mathbf{u}, z; \omega), \quad z_l < z < z_r, \quad \mathbf{u}(z_l) = \mathbf{u}_l$$

where $\mathbf{u} \in \mathbb{R}^2$. Fixed an ω, we can approximate $\mathbf{u}(z_r)$ by applying algorithms such as Runge-Kutta or Leap-frog.

Define F by $F(\mathbf{u}_l;\omega) = \tilde{v}(z_r;\omega)$. This function F takes in the initial value $\mathbf{u}_l$ and a fixed ω, and outputs the "landing point" $\tilde{v}(z_r;\omega)$. If ω is an eigenvalue of Eq.(3.4), then $\tilde{v}(z_r;\omega) = \tilde{v}_r$. Now we can find eigenvalues to Eq.(3.4) by solving the roots to the scalar equation

$$h(\omega) = F(\mathbf{u}_l;\omega) - \tilde{v}_r$$

Having this higher view of shooting method in mind, we first transform Eq.(1.9) to a IVP,

$$\begin{aligned} v' &= u \\ u' &= \frac{-1}{1-v_0^2}\left[\omega^2 v + 2i\omega(v_0 + v_0' v) - \left(3v_0 - \frac{1}{v_0}\right)v_0' u - \left(1 - \frac{1}{v_0}^2\right)(v_0')^2 v - \left(v_0 + \frac{1}{v_0}v_0'' v\right)\right] \end{aligned}$$

Since the singularity acts as a boundary condition, we can find the eigenvalues using the so-called shooting method. Starting from the singularity, we "shoot" the regular solution, found by using Frobenius method, to the left using the technique for IVP (initial value problem). By matching the end point value to the left boundary condition, we can determine the eigenvalues.

In order to get initially value for cases with transonic velocity profiles, we need the derivatives of $\tilde{v}$ at $z = 0$. Since we already have the power series expansion of $\tilde{v}$ near singularity. Thus, we can obtain the initial conditions from the coefficients,

$$\begin{aligned} v'(0) &= c_1 \\ u'(0) &= v''(0) = 2c_2 \end{aligned}$$

3.3.1 Result

By employing the shooting method, we are able to get eigenfunctions that crosses the singular point smoothly, see Fig.3.2. We have no freedom to choose boundary condition on the right, the left boundary and the singular point determine the flow entirely.

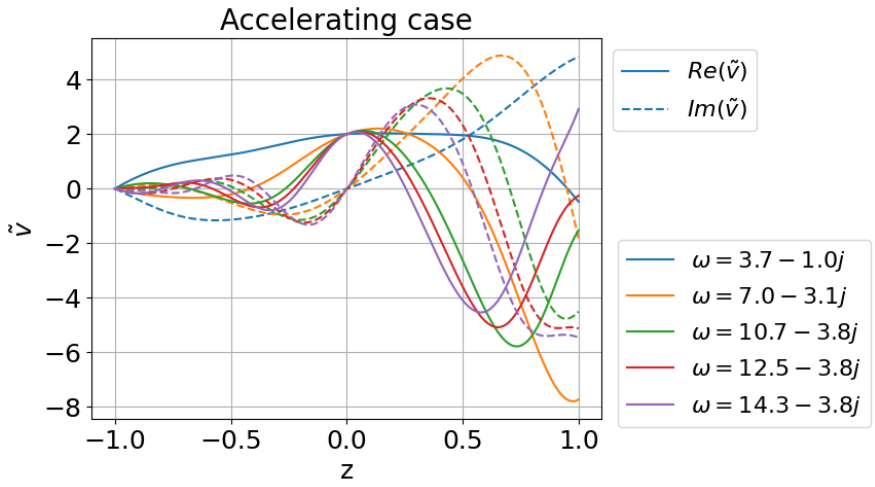

Figure 3.2: The solutions crosses the singular point smoothly. All modes are stable.

Chapter 4

Future Work

This research project can go to several direction.

- To improve the credibility of some results, different numerical calculation methods will be employed and confirmed with variational forms.
- Investigate and interpret the instability of an accelerating flow with non-zero left boundary values. See Fig.4.1
- Setup a analytically solvable problem with similar configuration. Compare the analytical results to the the experimental computations to better understand the physics.

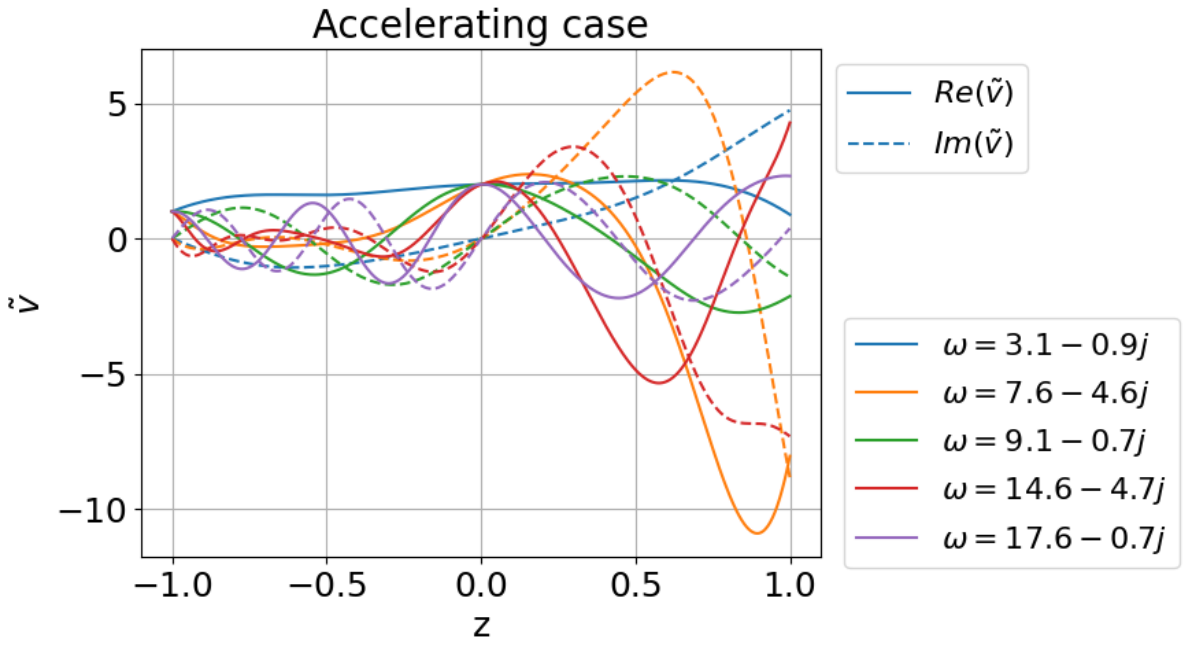

Figure 4.1: By matching the real part of the perturbation to a nonzero real value, we get different eigenvalues and eigenfunctions. What is the physical interpretation of "non-zero" boundary value? How do we interpret these eigenvalues?

Bibliography

[1] T. Aikawa. The stability of spherically symmetric accretion flows. *Astrophys Space Sci*, 66(2):277–285, Dec. 1979.

[2] F. F. Chen. *Introduction to Plasma Physics and Controlled Fusion*. Springer International Publishing, Cham, 2016.

[3] R. da Rocha. Black hole acoustics in the minimal geometric deformation of a de Laval nozzle. *The European Physical Journal C*, 77(5):355, 5 2017. [Online; accessed 2023-03-02].

[4] H. Furuhashi, Y. Nambu, and H. Saida. Simulation of an acoustic black hole in a Laval nozzle. *Class. Quantum Grav.*, 23(17):5417–5438, Sept. 2006.

[5] K. Jockers. On the stability of the solar wind. *Sol Phys*, 3(4):603–610, Apr. 1968.

[6] I. D. Kaganovich, A. Smolyakov, Y. Raitses, E. Ahedo, I. G. Mikellides, B. Jorns, F. Taccogna, R. Gueroult, S. Tsikata, A. Bourdon, J.-P. Boeuf, M. Keidar, A. T. Powis, M. Merino, M. Cappelli, K. Hara, J. A. Carlsson, N. J. Fisch, P. Chabert, I. Schweigert, T. Lafleur, K. Matyash, A. V. Khrabrov, R. W. Boswell, and A. Fruchtman. Physics of E $\times$ B discharges relevant to plasma propulsion and similar technologies. *Physics of Plasmas*, 27(12):120601, 12 2020.

[7] X. Llobet, K. Appert, A. Bondeson, and J. Vaclavik. On spectral pollution. *Computer Physics Communications*, 59(2):199–216, June 1990.

[8] A. I. Smolyakov, A. Sabo, P. Yushmanov, and S. Putvinskii. On quasineutral plasma flow in the magnetic nozzle. *Physics of Plasmas*, 28(6):060701, June 2021.

[9] L. N. L. N. Trefethen. *Spectral methods in MATLAB*. Software, environments, tools. Society for Industrial and Applied Mathematics, Philadelphia, PA, 2000.

[10] W. Unruh. Sonic analogue of black holes and the effects of high frequencies on black hole evaporation. *Physical review. D, Particles and fields*, 51(6):2827–2838, 1995.

Appendix A

Numerical Experiments

A.1 Constant Velocity Case - Subsonic

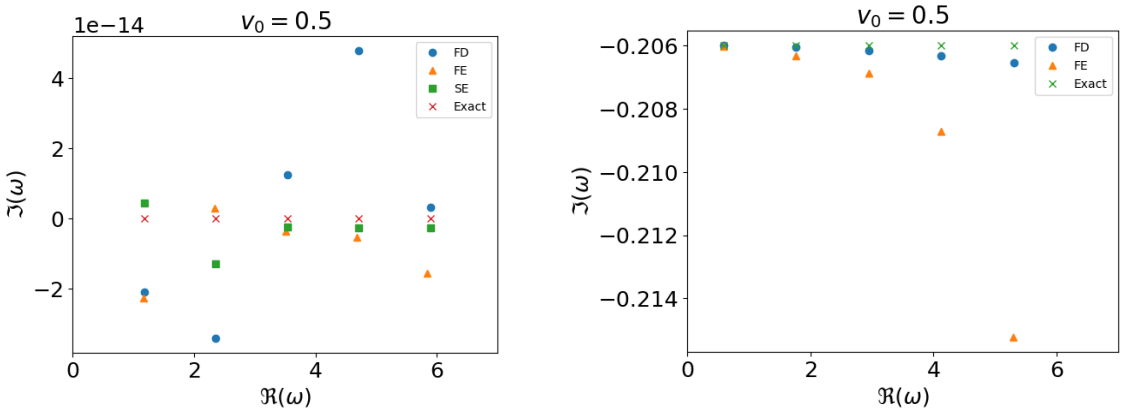

(a) Dirichlet boundary, all modes are stable.

(b) Fixed-open boundary, all modes are stable.

Figure A.1: Showing the first 5 eigenvalues. In the Dirichlet boundary case, all methods are close to the exact eigenvalues. Meanwhile, finite-difference method has higher accuracy than finite-element method in fixed-open case.

A.2 Constant Velocity Case - Supersonic

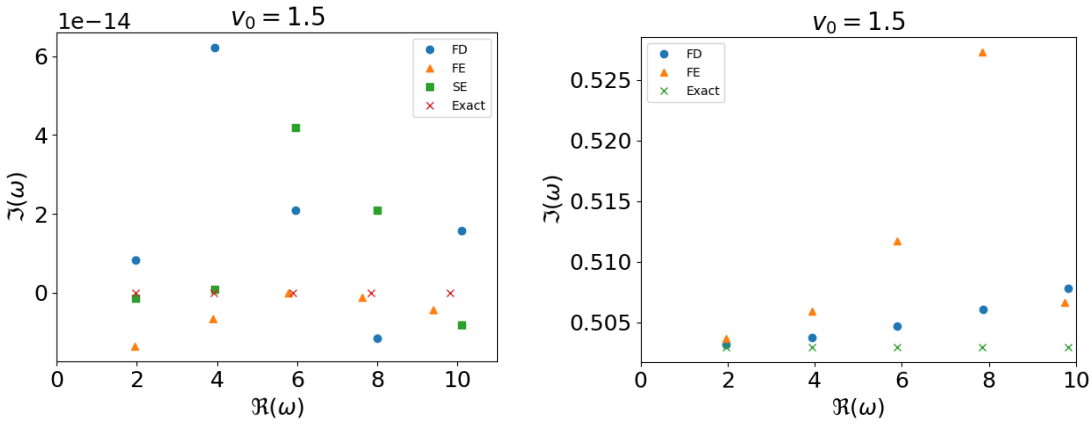

(a) Dirichlet boundary, filtered modes are stable. (b) Fixed-open boundary, all modes are unstable.

Figure A.2: Showing the first 5 eigenvalues. In the Dirichlet boundary case, all methods are close to the exact eigenvalues. Meanwhile, finite-difference method has higher accuracy than finite-element method in fixed-open case.

A.3 Error

Because the existence of exact solution to problems Eq.(1.9). The case with constant velocity profile is used as a sanity check. It allows us to verify the correctness of each method's implementation. This also serves as a reference to the accuracy spectral methods can achieve.

From Fig.A.1 and Fig.A.2, we see that the order of growth rates is about 10^{-14} for both subsonic and supersonic cases if the boundary condition is Dirichlet. We will use it a reference to the accuracy of our numerical methods. If a method produces growth rates with order close to 10^{-14}, we consider the growth rates to be 0.

Table A.1: Relative error of each eigenvalue.

$v_0 = 0.5$	1	2	3	4	5
FD	2.827e-05	1.130e-04	2.541e-04	4.512e-04	7.040e-04
FE	0.005	0.005	0.006	0.008	0.010
SE	2.896e-05	1.157e-04	2.603e-04	4.626e-04	7.217e-04

$v_0 = 1.5$	1	2	3	4	5
FD	0.001	0.005	0.010	0.019	0.030
FE	0.006	0.010	0.019	0.029	0.043
SE	0.001	0.005	0.011	0.019	0.030

Table A.2: Relative error of each eigenvalue. Notice that the ground mode for subsonic case is non-zero.

$v_0 = 0.5$	0	1	2	3	4
FD	1.209e-05	3.458e-05	5.775e-05	8.153e-05	1.061e-04
FE	8.090e-05	2.007e-04	2.981e-04	6.596e-04	1.821e-03

$v_0 = 1.5$	1	2	3	4	5
FD	9.163e-05	2.435e-04	4.833e-04	8.160e-04	1.243e-03
FE	4.431e-04	7.924e-04	1.516e-03	3.103e-03	8.001e-03

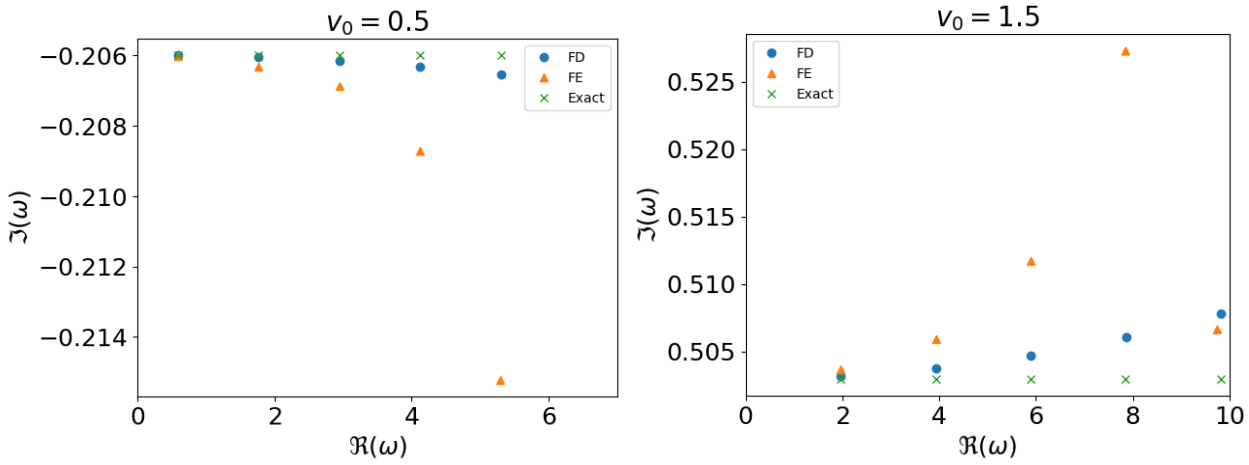

(a) All modes are stable.

(b) All modes are unstable.

Figure A.3: Showing the first 5 eigenvalues of each method. Finite-difference method has much better accuracy than finite-element method.

A.4 Subsonic Case

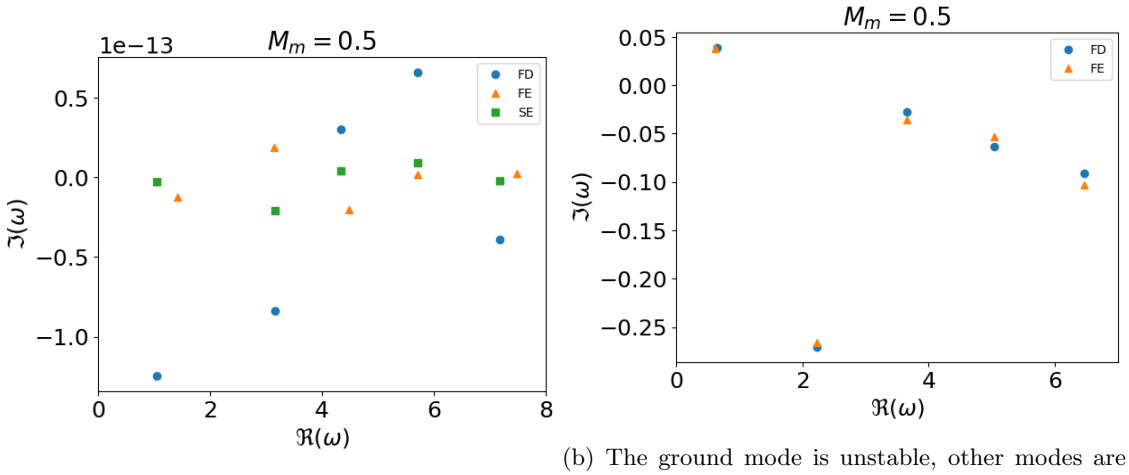

(a) Dirichlet boundary, all modes are stable.

(b) The ground mode is unstable, other modes are stable.

Figure A.4: Showing the first 5 modes. It suggests that the subsonic flow in magnetic nozzle is stable.

A.5 Supersonic Case

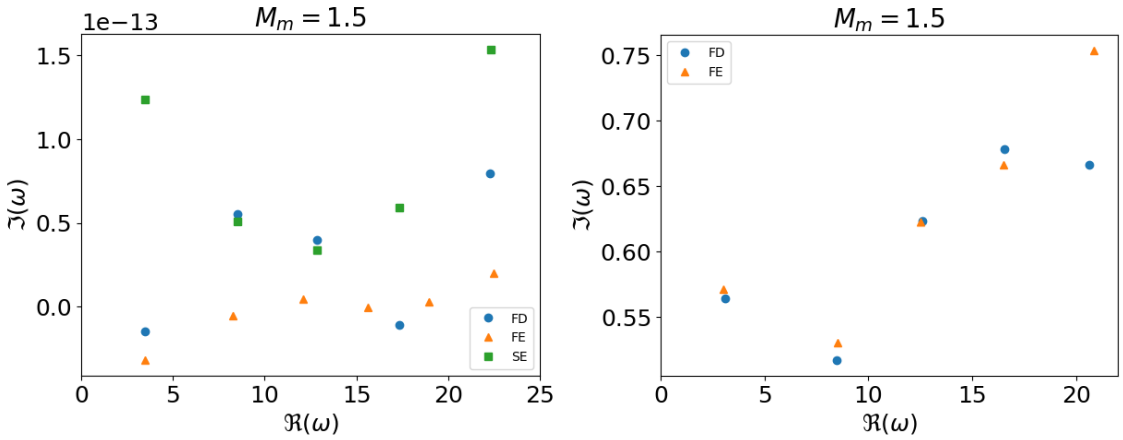

(a) Dirichlet boundary, filtered modes are stable. (b) Fixed-open boundary, all modes are unstable.

Figure A.5: This suggests that the supersonic flow is stable if the boundary is Dirichlet and unstable if the boundary is left-fixed-right-open.

A.6 Accelerating Case

Starting from the singular point, we shoot the solution to the left boundary. We find the set of eigenvalues such that $\tilde{v}(-1) = 0$. With these eigenvalues, we can extend the solution to the supersonic region $(0, 1]$. The first five eigenvalues are drawn in the graph.

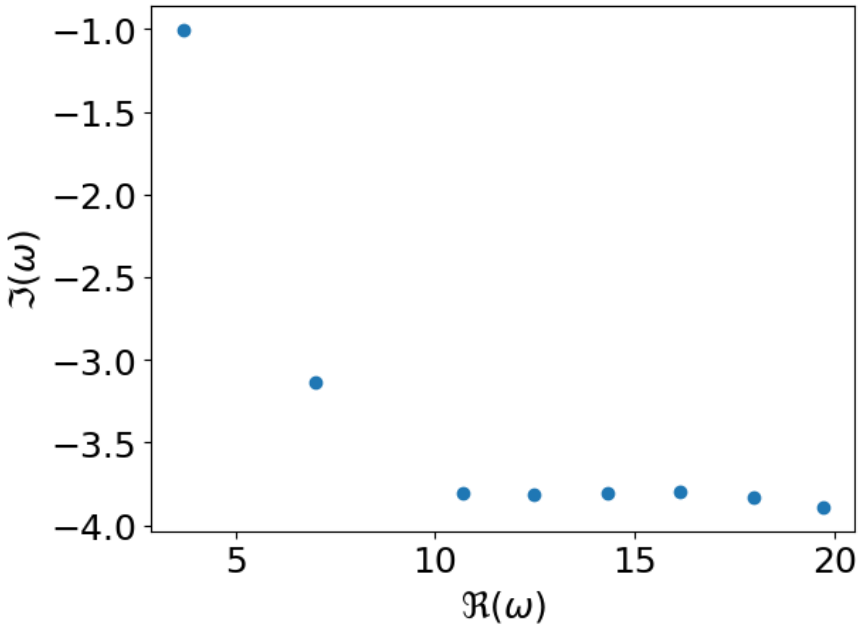

Figure A.6: All modes are stable.

Appendix B

Spectral Pollution: Analysis of Numerical Spectrum

If we assume $v \sim \exp(ikx)$, and let $\beta \equiv kh/2$. Then in finite difference discretization scheme, the differential operators $\mathrm{d}^n/\mathrm{d}z^n$ are equivalent to the following factors [7],

$$\begin{aligned} G_0 &= 1 \\ G_1 &= [\exp(2i\beta) - \exp(-2i\beta)]/2h = (i/h)\sin(2\beta) \\ G_2 &= [\exp(2i\beta) - 2 - \exp(-2i\beta)]/h^2 = (2/h^2)(\cos(2\beta) - 1) \end{aligned} \tag{B.1}$$

Using the G-operator, Eq.(B.1), the discretized equation of Eq.(2.2) is

$$(\omega^2 G_0 + \omega G_1 + G_2)\tilde{\mathbf{v}} = 0 \tag{B.2}$$

where $\tilde{\mathbf{v}}$ is the discretized vector of $\tilde{v}$.

Solving Eq.(B.2), we obtain the numerical dispersion relation,

$$\omega = \frac{2\sin(\beta)}{h}\left(v_0 \pm \sqrt{1 - v_0^2 \sin^2(\beta)}\right) \tag{B.3}$$

Given h (fixed the mesh resolution), we see that

- ω is real for all k if $v_0 < 1$.
- ω is complex for large k, more specifically $k > h/2 \arcsin(1/v_0)$, if $v_0 > 1$.
- For small k, meaning $k \to 0$, Eq.(B.3) is a good representation for the analytical dispersion relation, Eq.(2.3).

This explains why the spurious unstable modes occur when $v_0 > 1$.

One way to filter the spurious modes is to remove all modes with $k > h/2 \arcsin(1/v_0)$. However, this is not a good way to deal with general cases because it requires the solution to the discretized problem Eq.(B.2). For general problem with non-constant velocity profile, it is hard to solve the discretized problem directly.